RESEARCH PAPER

Histopathological and Immunohistochemical Evaluation of Paclitaxel in DMBA-Induced Mammary Carcinogenesis in Female Rats

Zeinab M. Abd Elrahman[1*], Dalia A. Shabaan[1], Amany Hassan [2], Shehab Hafez Mohamed[1], Sanaa Ahmed El-Sherbiny[1]

1. *Department of Medical Histology and Cell Biology, Faculty of Medicine, Mansoura University.*
2. *Department of Anatomic Pathology, Faculty of Medicine, Mansoura University.*

Received: 24th June, 2026; Revised: 25th July, 2026; Accepted: 27th July, 2026; Available Online: 04th August, 2026

ABSTRACT

Breast cancer is a common malignant tumor globally. Experimental models such as DMBA-induced mammary carcinogenesis are broadly utilized to study tumor development and therapeutic response. Paclitaxel is a naturally derived chemotherapeutic agent broadly used in management of various cancers. This study aimed to evaluate the histopathological and immunohistochemical effects of paclitaxel on DMBA-induced mammary carcinogenesis in rats. Forty female albino rats were divided into three groups. Group I served as a control group. Group II was the DMBA-induced carcinogenesis group and received DMBA (50 mg/kg) dissolved in corn oil via oral gavage once weekly for four weeks, starting at 55 days of age. Group III received DMBA plus paclitaxel (33 mg/kg) intraperitoneal once weekly for four weeks, starting at 16th week of experiment. When the experiment was ended, tissue samples were processed. Light microscopic study was performed. Morphometric and statistical studies were conducted. DMBA induced marked histopathological alterations ranging from DCIS to IDC, accompanied by increased ER & Ki-67 expression. Treatment with paclitaxel improved tissue architecture and decreased ER and Ki-67 expression. HER2 expression was negative in all the control and experimental groups. Paclitaxel exerted therapeutic effect against DMBA-induced mammary carcinogenesis and resulted in marked improvement of tissue architecture of the mammary gland. This proved that paclitaxel was a potent chemotherapeutic agent.

Key words: DMBA, Paclitaxel, DCIS, IDC, ER, Ki67, HER2.

How to cite this article: Abd Elrahman Z.M, Shabaan D.A, Hassan A, Mohamed S.H, El-Sherbiny S.A, Histopathological and Immunohistochemical Evaluation of Paclitaxel in DMBA-Induced Mammary Carcinogenesis in Female Rats. 2026;16(73s): 948-961. DOI: 10.25258/ijddt.16.73s.104

Source of support: None

Conflict of interest: None

INTRODUCTION

Breast cancer is a major public health problem. It is the most commonly diagnosed malignant tumor globally. The World Health Organization, demonstrated that over two million new cases of breast cancer are diagnosed each year [1,2]. It is the commonest cancer in females globally, representing 24.2% of all malignant tumor cases among females [3]. In addition, it represents the main cause of cancer death in females, with more than 680000 deaths per year [1,2].

7,12- Dimethyl Benz (a) Anthracene (DMBA) is a polycyclic aromatic hydrocarbon, produced during the incomplete combustion of carbon-containing compounds. It is predominantly found in tobacco smoke, wood smoke and motor vehicle exhaust emissions [4]. It is an immunosuppressor and a powerful organ specific laboratory carcinogen. The main target sites for the potent carcinogenicity of DMBA are the skin and the mammary gland, so it is commonly used as an inducing agent that develops mammary carcinoma in the animal model [5,6]. DMBA-induced mammary tumors in female rats represent a reliable experimental model that closely mimics human breast cancer in many aspects, such as morphology and hormone responsiveness [7,8].

Paclitaxel is a broadly used chemotherapeutic agent in cancer treatment due to its potent antitumor activity. It is a natural agent derived from the bark of the Pacific yew tree (Taxus brevifolia). It is commonly utilized in the management of several malignant tumors, such as ovarian, lung, breast, head and neck cancers [9]. Paclitaxel is also preferred in other malignancies that are refractory to conventional chemotherapy. These types include previously treated lymphoma, small-cell lung cancers, esophageal, gastric, endometrial, bladder cancers, malignant germ cell tumors, and AIDS-associated Kaposi's sarcoma [10]. Its anticancer effect is mainly related to stabilization of microtubules, causing suppression of cell division and triggering of apoptosis induction [11]. Despite its clinical efficacy, paclitaxel is accompanied by some adverse events, which may restrict its therapeutic use [12].

Despite advances in diagnosis and treatment, breast cancer remains a prevalent malignant tumor worldwide among females [1]. So, we aimed to assess the histopathological and immunohistochemical changes in the mammary gland of adult female albino rats following administration of DMBA and to assess the potential ameliorative effect of paclitaxel on DMBA-induced changes in rat mammary gland.

**Author for Correspondence:* zeinababdelrahman@mans.edu.eg *ORCID ID: 0000-0003-3864-8171.*

MATERIAL AND METHODS:

Chemicals:

1. **DMBA:** Imported by the Egyptian International Center for Import in Cairo, Egypt, from SIGMA-ALDRICH in St. Louis, Missouri, USA. Corn oil was used to dissolve it before use.
2. **Paclitaxel:** Commercial paclitaxel will be used (unitaxel) from Emic pharmaceuticals, Cairo, Egypt.

Place of the study:

The current experimental study was conducted in Medical Experimental Research Centre (MERC), Mansoura University based on global guidelines for care and use of laboratory animals. Approval of the Mansoura University IRB was obtained.

Duration of the experiment: 20 weeks.

Animals: Forty female albino rats, 40 days old, ranging in weight from 90-120 gm, were acquired from animal house, faculty of medicine, Mansoura university. The animals were housed in in metal cages with soft wood chips. All rats were maintained at optimal environmental conditions (25 °C temperature and 70% humidity with 12-h light/dark cycle) and have free access to food and water. Rats were acclimatized for two weeks and the experiment started at 55th day of age.

- **The rats were randomly divided into three equal groups:**

Group I (control group) (N=10):

Rats were subdivided into **two equal subgroups:**

1. **Subgroup IA: (negative control):** five rats on standard diet and were not given any drugs.
2. **Subgroup IB:** five rats were given only corn oil by oral gavage once a week for 4 weeks.

Group II (DMBA-induced carcinogenesis) (N=15):

- Fifteen rats were given DMBA at a dose (50 mg/kg) dissolved in corn oil by oral gavages every week for four weeks starting at 55th day of age [13, 14].
- The mammary glands of the rats were palpated every week four weeks after the last dose of DMBA to detect the appearance of breast masses [14, 15].
- At 16th week following the initial dose of DMBA, all rats developed mammary gland masses.

Group III (DMBA-induced carcinogenesis given paclitaxel) (N=15):

- Fifteen rats were given DMBA at the same dose plus paclitaxel intraperitoneal at a dose (33mg/kg) once a week for four weeks starting at 16th week of experiment [16].
- At the end of the experiment, the control and matching experimental groups were sacrificed under intraperitoneal anaesthesia by using sodium pentobarbital (40 mg/kg) [17]. Dissection of the mammary glands was conducted and then prepared for light microscopy.

Light Microscopic Study:

Samples from the mammary gland were fixed in 10% neutral buffered formalin and processed using the traditional protocol to produce paraffin sections. Tissue preparation was done by gradual dehydration by utilizing ascending grades of alcohol. Then, xylene was used to clear the samples, and embedding in soft then hard paraffin wax was done. Paraffin sections (4-5 µm) were acquired and stained with hematoxylin and eosin (H&E) stain [18] for routine histologic examination. Immunohistochemical staining was used to stain some sections to demonstrate the ER, Ki-67 and HER2 immune reactions[19].

Immunohistochemistry methodology of ER, Ki-67 and HER2:

Regarding immunohistochemical study, the deparaffinized 5 µm paraffin sections were mounted on coated slides to localize ER, Ki-67 and HER2 using avidin–biotin-complex (ABC) immunoperoxidase approach. The sections were incubated in hydrogen peroxide for 15 min to inhibit the endogenous peroxidase activity then slides were washed in phosphate buffered saline (PBS) solution for 10 min. Antigen retrieval was performed by putting the slides in citrate buffer (pH 6), followed by heating them in a microwave oven at 100°c for 10 min. The sections were incubated with the primary antibodies; anti-ER and anti-Ki67 (dilution 1:200) and anti HER2 (dilution 1:100) for one hour at 22°C. The primary antibody used for ER-α was a rabbit polyclonal antibody, class IgG (catalog number: bs-3130R, Bioss Inc., Woburn, Massachusetts, USA). For KI-67, a rabbit polyclonal antibody, class IgG (catalog number: bs-2130R, Bioss Inc., Woburn, Massachusetts, USA) was utilized. For HER2, a rabbit polyclonal antibody, class IgG (catalog number: A2071, ABclonal, Woburn, USA) was used. The primary antibodies were determined with the anti-rabbit biotinylated secondary antibody (1:200, PK-4001; Chinese Fir Golden Bridge Company). Two drops of the secondary antibody, prepared at a dilution of 1:200 in 1% bovine serum albumin (BSA) dissolved in phosphate-buffered saline (PBS), were applied to the slides, and followed by incubation at room temperature for 10 min to avoid non-specific background staining. Visualization of immunoreactivity was achieved using 3,3′-diaminobenzidine (DAB) as chromogen for 5–10 min, yielding a brown reaction at antigen sites. Mayer's Hematoxylin was used as a counterstain [20]. Negative control slides were included in Tris-buffered saline instead of the primary antibodies. Positive control sections were prepared from human uterus for ER[21], human colon for ki-67 [22] and human invasive carcinoma for HER2 [23], according to manufacturer company of the primary antibody. For ER and Ki-67; a brown nuclear immune reaction was considered positive. For HER2; a brown membranous immune reaction was considered positive.

Histomorphometric Study:

Slides were photographed using a ToupCam digital camera (XCAM1080PHA; 2.8 pixels, UK) attached to an Olympus® microscope (CX23LEDRF; Japan), with 0.5 X photo adaptor. The percentage area of positive immunoreactivity for ER and Ki-67 was evaluated in ER- and Ki-67-stained sections, respectively, under high-power fields (HPF, ×400). Six non-overlapping microscopic fields were randomly chosen for morphometric assessment. The generated photos were

analyzed on an Intel® Core I7®-based computer using Video Test Morphology® software (Russia), which has a specific built-in mechanism for calibrated distance measurement, area measurement, automatic object analysis, and color intensity.

Statistical Study:

Morphometric data were coded, computed, tabulated, and analyzed using the computer program SPSS (Statistical package for social science) version 26. Data were presented as mean ± standard deviation (SD) or median as appropriate. One-way analysis of variance (ANOVA) test was used to compare more than two groups of parametric (numerical) data, followed by post-hoc Tukey test for multiple comparisons [24]. P-value ≤ 0.05 was considered statistically significant. Blinded statistical analysis was performed, where both microscopists and data analyzers were unaware of the study design and groups.

RESULTS:

N.B: Four rats from group II and one rat from group III died with mortality rate 26.7% and 6.67% respectively.

I) Light Microscopic Results:

(1) Hematoxylin and Eosin (H&E) Stain:

Group I (Control Group):

Examination of sections of the mammary gland of the control group showed the same structure of the subgroups (IA and IB). Photomicrographs of subgroup IA were used to represent the control group.

Examination of sections of the rat mammary gland of the control group I revealed mammary glands arranged in lobules. The lobules were composed of ducts and few alveoli, encircled by a minimal amount of connective tissue containing fibroblasts. An abundant content of adipose connective tissue was present in between different ducts and alveoli. The adipocytes in the surrounding adipose connective tissue contained a large lipid globule and flattened peripheral nucleus. The blood vessels were normal. The mammary ducts were lined with a layer of cubical epithelial cells and encircled by a layer of myoepithelial cells. Cuboidal epithelial cells lined the alveoli **(Figure 1A & 1B).**

Group II (DMBA-induced carcinogenesis):

Examination of sections of the mammary gland revealed invasive ductal carcinoma (IDC) and ductal carcinoma in situ (DCIS). Intermediate-grade DCIS specimens showed distended ducts lined by neoplastic cells arranged in a cribriform pattern. The neoplastic cells exhibited intermediate-grade cytological atypia, characterized by moderate nuclear pleomorphism. Some nuclei appeared hyperchromatic and some were vesicular with prominent nucleoli. The surrounding stroma showed fibrosis with areas of fat necrosis **(Figure 1C & 1D).**

High-grade DCIS specimens showed loss of the normal architecture. Distended ducts were lined by neoplastic cells arranged in a cribriform pattern. The neoplastic cells exhibited high-grade cytological atypia, characterized by marked nuclear pleomorphism. Some nuclei appeared hyperchromatic and some were vesicular with prominent nucleoli. The surrounding stroma showed fibrosis **(Figure 1E & 1F).** Mitotic figures were also observed **(Figure 1E).**

IDC specimens showed infiltration of the stroma by malignant neoplastic proliferating cells arranged predominantly in the form of tubular structures and solid sheets. The cells exhibited mild pleomorphism with hyperchromatic nuclei. The stroma showed desmoplastic reaction {stromal fibrosis associated with malignant cells} with areas of fat necrosis **(Figure 1G & 1H).**

Group III (DMBA-induced carcinogenesis given paclitaxel):

There were no evidence of IDC or DCIS. Examination of sections of the mammary gland revealed that the ducts were lined by cubical epithelial cells and surrounded by a layer of myoepithelial cells. The connective tissue surrounding the ducts contained normal fibroblasts Adipose connective tissue was present without necrosis. Normal blood vessels could be seen **(Figure 2A, 2B, 2C & 2D).** Connective tissue contained some degenerated fibroblasts with atypical enlarged hyperchromatic nuclei. The alveoli were composed of cuboidal epithelial cells **(Figure 2A& 2B).** Some ducts were Slightly dilated with areas of stratification. Some areas of the stroma exhibited inflammatory infiltrate and fibrosis **(Figure 2C & 2D).**

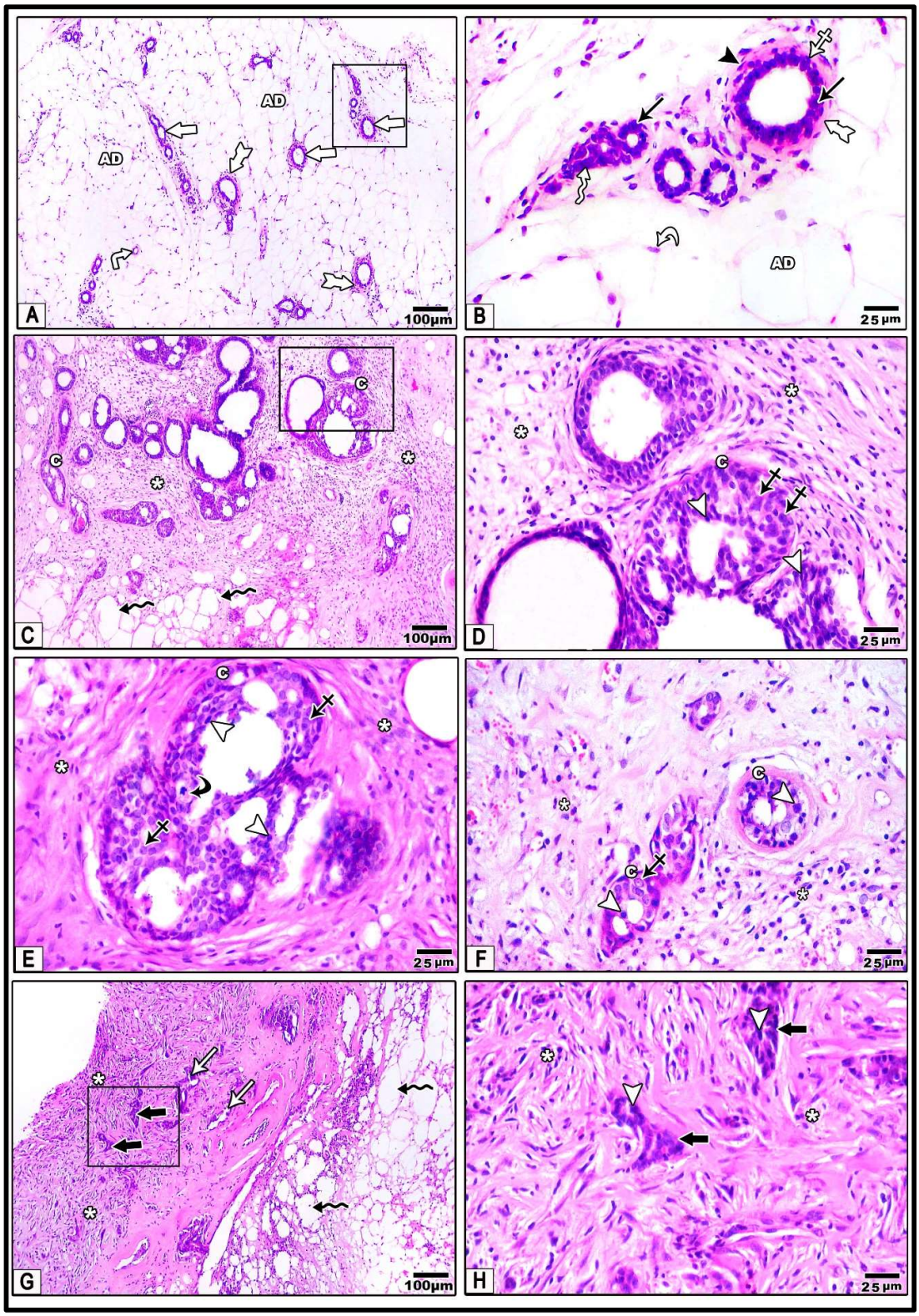

Figure 1: Mammary gland sections stained with H & E **(A–B) Control group I** shows scattered mammary ducts (white thick arrows) lined by a layer of cuboidal epithelial cells (black arrows) and an outer myoepithelial layer (white crossed arrow). The ducts are embedded in connective tissue (white bifid arrows) containing fibroblasts (black arrowhead). Adipose tissue shows adipocytes (AD) with a large lipid globule and peripherally flattened nucleus (white curved arrow). Alveoli are lined by cuboidal epithelial cells (white zigzag arrow). Normal blood vessels are also observed (angled arrow). (**C–H**

group II; DMBA-induced carcinogenesis) (C–D) Distended ducts are lined by neoplastic cells arranged in a cribriform pattern (C). The neoplastic cells exhibit intermediate-grade atypia with moderate pleomorphism, hyperchromasia (white arrowheads), vesicular nuclei with prominent nucleoli (black crossed arrows). The stroma exhibits fibrosis (asterisks) and fat necrosis (black zigzag arrows). These features are consistent with intermediate-grade DCIS. (**E)** loss of normal architecture and irregular distention of the affected duct. It is lined by neoplastic cells arranged in a cribriform pattern (C). The neoplastic cells exhibit high-grade cytological atypia, characterized by marked nuclear pleomorphism with hyperchromasia (white arrowheads), and some vesicular nuclei (black crossed arrows). Mitotic figure can be seen (black curved arrow). The surrounding stroma shows fibrosis (asterisks). These features are consistent with high-grade DCIS. **(F)** The affected duct is occupied by neoplastic cells arranged in a cribriform pattern (C). The neoplastic cells exhibit high-grade cytological atypia, marked nuclear pleomorphism with hyperchromasia (white arrowheads), and some vesicular nuclei (black crossed arrow). The surrounding stroma showing fibrosis (asterisks). The features are consistent with high-grade DCIS. (**G–H)** Show stromal invasion by malignant neoplastic proliferating cells arranged in tubular structures (white arrows) and solid sheets (black thick arrows). The cells show mild pleomorphism with hyperchromatic nuclei (white arrowheads). The stroma showed desmoplastic reaction (asterisks) and areas of fat necrosis (black zigzag arrows). These features are consistent with IDC.

(H & E A, C, G x100, B, D, E, F, H x400)

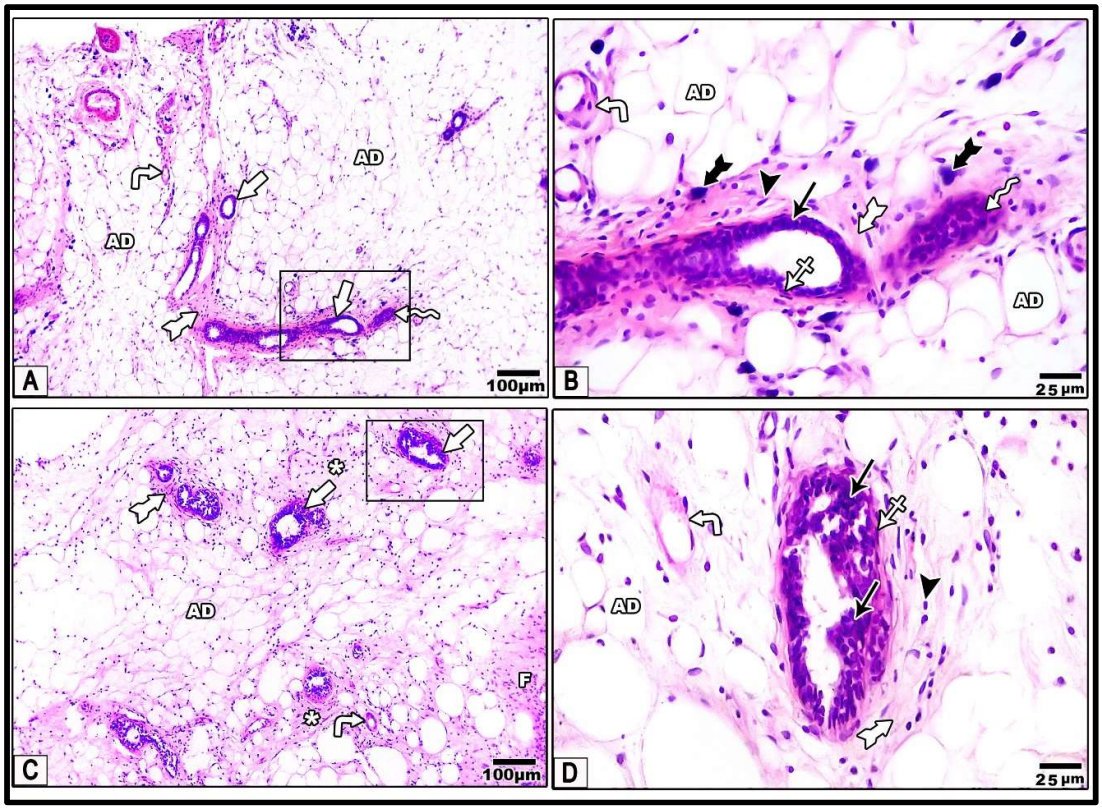

Figure 2: Mammary gland sections stained with H & E **(A–D group III; DMBA-induced carcinogenesis given paclitaxel)** (**A–B**) Mammary ducts (white thick arrows) are lined by cubical ductal epithelial cells (black arrow) and surrounded by a layer of myoepithelial cells (white crossed arrow). The ducts are surrounded by connective tissue (white bifid arrows) containing normal fibroblasts (black arrowhead) and degenerated fibroblasts with atypical enlarged hyperchromatic nuclei (black bifid arrows). The alveolus (white zigzag arrows) is composed of cuboidal epithelial cells. Adipose tissue (AD) is present in between the ducts and alveoli. Note the normal blood vessels (angled arrows). (**C–D**) Slightly dilated mammary ducts (white thick arrows) are lined by cubical ductal epithelial cells with areas of stratification (black arrows) and surrounded by a layer of myoepithelial cells (white crossed arrow). The ducts are surrounded by connective tissue (white bifid arrow) containing fibroblasts (black arrowhead) Adipose tissue (AD) is present in between the ducts. The surrounding stroma shows areas of inflammatory cellular infiltrate (F) and fibrosis (asterisks). Note the normal blood vessels (angled arrows).

(H & E A, C x100, B, D x400)

(2) Immunehistochemical Results:

a-ER-Immune Reaction:

Group I (control):

Examination of ER-immunostained sections of the mammary gland showed nuclear ER positive immunoreaction in some cells lining the ducts and the alveoli **(Figure 3A).**

Group II (DMBA-induced carcinogenesis):

Examination of ER-immunostained sections of the mammary gland showed DCIS specimens exhibiting nuclear ER positive immunoreaction in most of the neoplastic epithelial cells lining the affected ducts **(Figure 3B).** A similar reaction pattern was observed in IDC specimens **(Figure 3C).**

Group III (DMBA-induced carcinogenesis given paclitaxel):

Examination of ER-immunostained sections of the mammary gland showed nuclear ER positive immunoreaction in few cells lining the ducts and alveoli **(Figure 3D & 3E).**

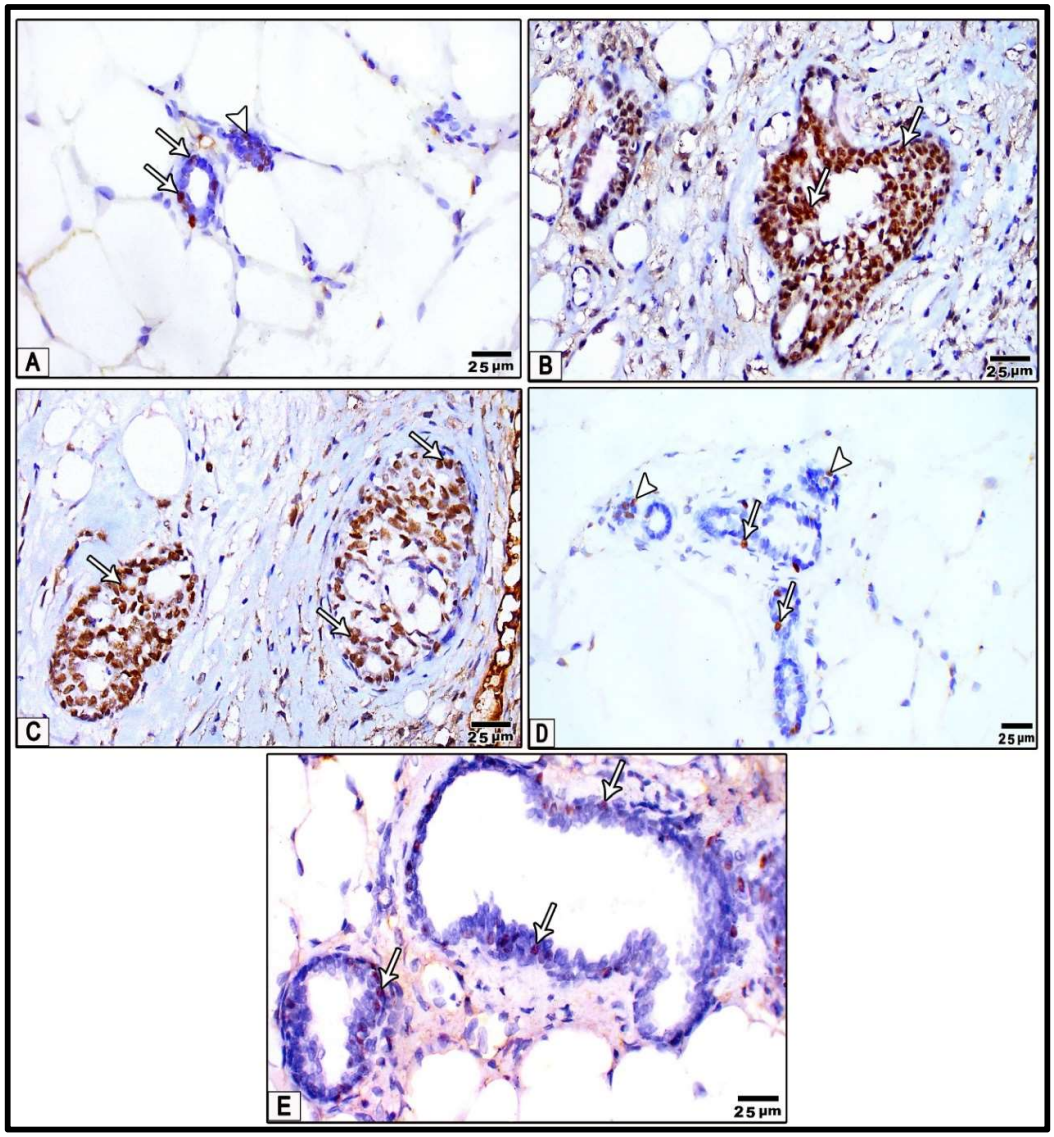

Figure 3: ER expression in immunohistochemically stained mammary gland sections **(A) Control group I** shows nuclear ER positive immunoreaction in some cells lining the ducts (arrows) and the alveoli (arrowhead). (**B–C group II; DMBA-induced carcinogenesis). (B)** DCIS shows nuclear ER positive immunoreaction in most of the neoplastic epithelial cells lining the affected duct (arrows). **(C)** IDC shows nuclear ER positive immunoreaction in most of the malignant neoplastic epithelial cells lining the ducts arranged in tubules (arrows) **(D-E) Group III (DMBA-induced carcinogenesis given paclitaxel)** shows nuclear ER positive immunoreaction in few cells lining the ducts (arrows) and the alveoli (arrowheads). **(IHC for ER A-E x400)**

b-ki-67-Immune Reaction:

Group I (control):

Examination of Ki-67 immunostained sections of the mammary gland showed nuclear Ki-67 positive immunoreaction in only few cells lining the ducts and the alveoli **(Figure 4A).**

Group II (DMBA-induced carcinogenesis):

Examination of Ki-67 immunostained sections of the mammary gland showed DCIS specimens exhibiting nuclear Ki-67 positive immunoreaction in some neoplastic epithelial cells lining the affected duct and also some cells of the stroma **(Figure 4B).** A similar reaction pattern was observed in IDC specimens **(Figure 4C).**

Group III (DMBA-induced carcinogenesis given paclitaxel):

Examination of Ki-67 immunostained sections of the mammary gland showed nuclear Ki-67 positive immunoreaction in few cells lining the ducts and alveoli **(Figure 4D & 4E).**

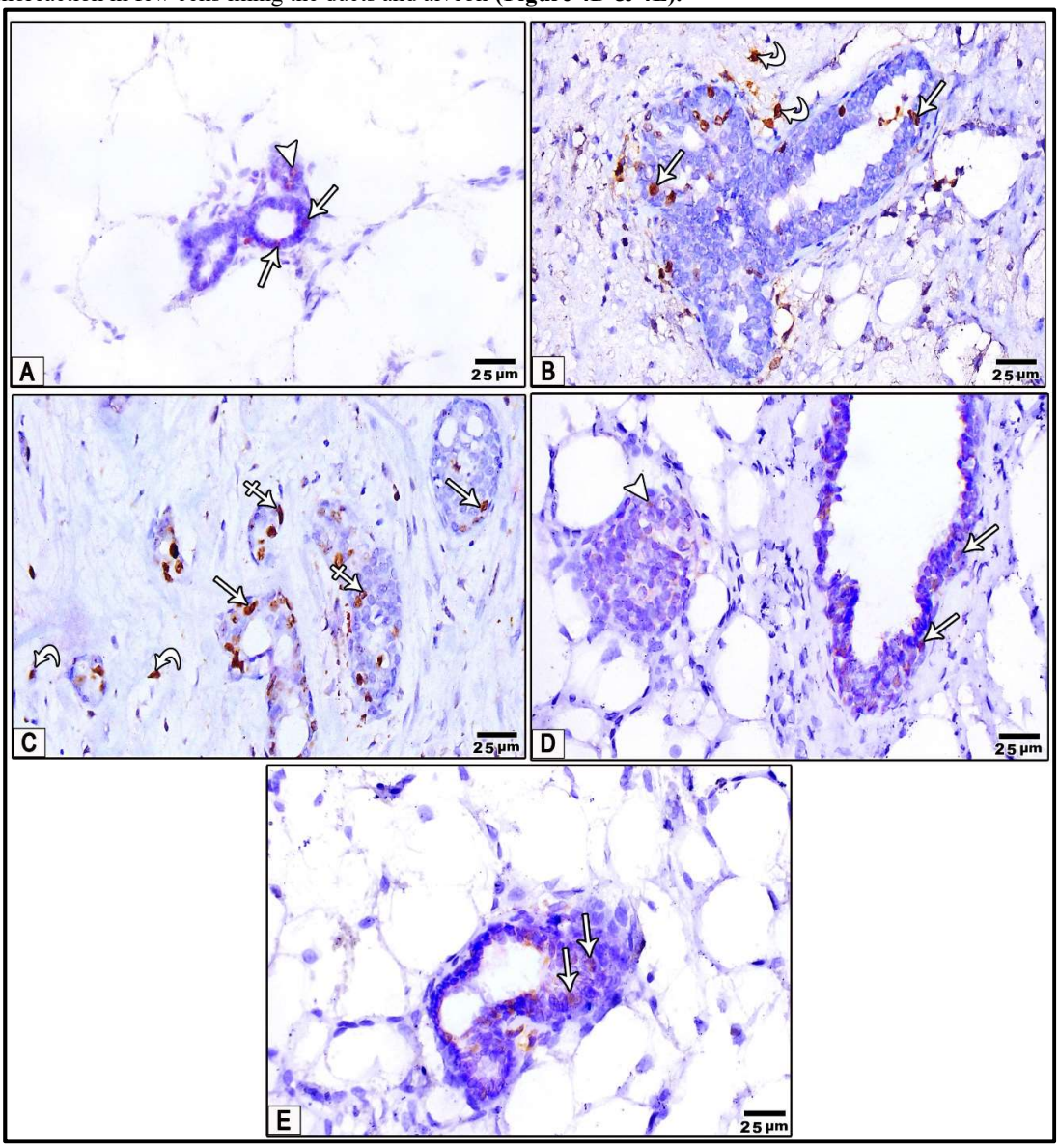

Figure 4: Ki-67 expression in immunohistochemically stained mammary gland sections **(A) Control group I** shows nuclear ki-67 positive immunoreaction in few cells lining the ducts (arrows) and the alveoli (arrowhead). (**B–C group II; DMBA-induced carcinogenesis). (B)** DCIS shows nuclear ki-67 positive immunoreaction in some neoplastic epithelial cells lining the affected duct (arrows). Some positive cells are also present in the stroma (curved arrows) **(C)** IDC shows nuclear ki-67 positive immunoreaction in some malignant neoplastic epithelial cells lining the ducts arranged in tubules (arrows) and solid sheets (crossed arrows). Some positive cells are also present in the stroma (curved arrows) **(D-E) Group**

III (DMBA-induced carcinogenesis given paclitaxel) shows nuclear ki-67 positive immunoreaction in few cells lining the ducts (arrows) and the alveoli (arrowhead).

(IHC for Ki-67 A-E x400)

c-HER2-Immune Reaction:

Group I (control):

Examination of HER2 immunostained sections of the mammary gland showed HER2 negative immunoreaction in the cells lining the ducts and the alveoli **(Figure 5A).**

Group II (DMBA-induced carcinogenesis):

Examination of HER2 immunostained sections of the mammary gland showed DCIS specimens exhibiting HER2 negative immunoreaction in the neoplastic epithelial cells lining the affected ducts **(Figure 5B).** A similar reaction pattern was observed in IDC specimens **(Figure 5C).**

Group III (DMBA-induced carcinogenesis given paclitaxel):

Examination of HER2 immunostained sections of the mammary gland showed HER2 negative immunoreaction in the cells lining the ducts and alveoli **(Figure 5D).**

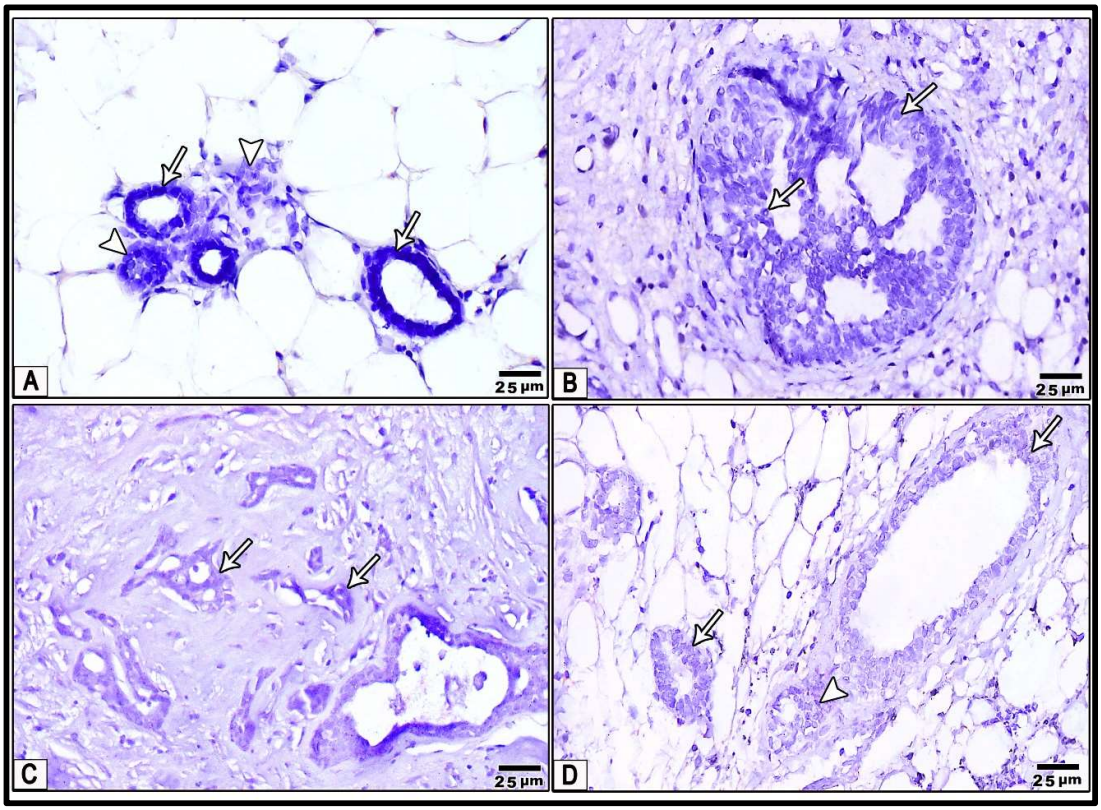

Figure 5: HER2 expression in immunohistochemically stained mammary gland sections **(A) Control group I** shows HER2 negative immunoreaction in the cells lining the ducts (arrows) and the alveoli (arrowheads). (**B–C group II; DMBA-induced carcinogenesis). (B)** DCIS shows HER2 negative immunoreaction in the neoplastic epithelial cells lining the involved duct (arrows). **(C)** IDC shows HER2 negative negative immunoreaction in the malignant neoplastic epithelial cells lining the ducts arranged in tubules (arrows). **(D-E) Group III (DMBA-induced carcinogenesis given paclitaxel)** shows HER2 negative immunoreaction in the cells lining the ducts (arrows) and the alveoli (arrowhead).

(IHC for HER2 A-E x400)

I) Statistical Results:

- **Percentage area of ER positive immune-reaction at a magnification x400 in the control and experimental groups:**

As regard the control group (I), subgroup IA (0.509±0.15) and subgroup IB (0.475±0.20) showed insignificant (P=1) difference in the percentage area of ER positive immune-reaction. As compared to control group (IA and IB), a high significant increase in the percentage area of ER positive immune-reaction was noticed in group II (8.214±1.17, P<0.001). Furthermore, a significant (P =0.002 and 0.001) increase in the percentage area of ER positive immune-reaction was noticed

in group III (2.031 ± 0.21), as compared to control group (IA and IB). In addition, group III showed a high significant (P<0.001) decrease in the percentage area of ER positive immune-reaction, as compared to group II **(Table 1 and Histogram 1).**

Table (1): Percentage (%) area of ER positive immune-reaction (mean±SD) in the control and experimental groups:

	Group I (Control)		Group II (DMBA)	Group III (DMBA+ Paclitaxel)	Test of significance (ANOVA)
	Subgroup IA	Subgroup IB			
Mean ± SD	0.509 ± 0.15	0.475 ± 0.20	8.214 ± 1.17	2.031 ± 0.21	P < 0.001**
P_1		1.0	<0.001**	0.002*	
P_2			<0.001**	0.001*	
P_3				<0.001**	

6 replicas in each group, SD: Standard Deviation, P for ANOVA test.
* Statistically significant if P ≤0.05.
**Highly statistically significant result if P ≤0.001.
P_1: comparison in relation to group IA (Control).
P_2: comparison in relation to group IB (Control).
P_3: comparison in relation to group II (DMBA).

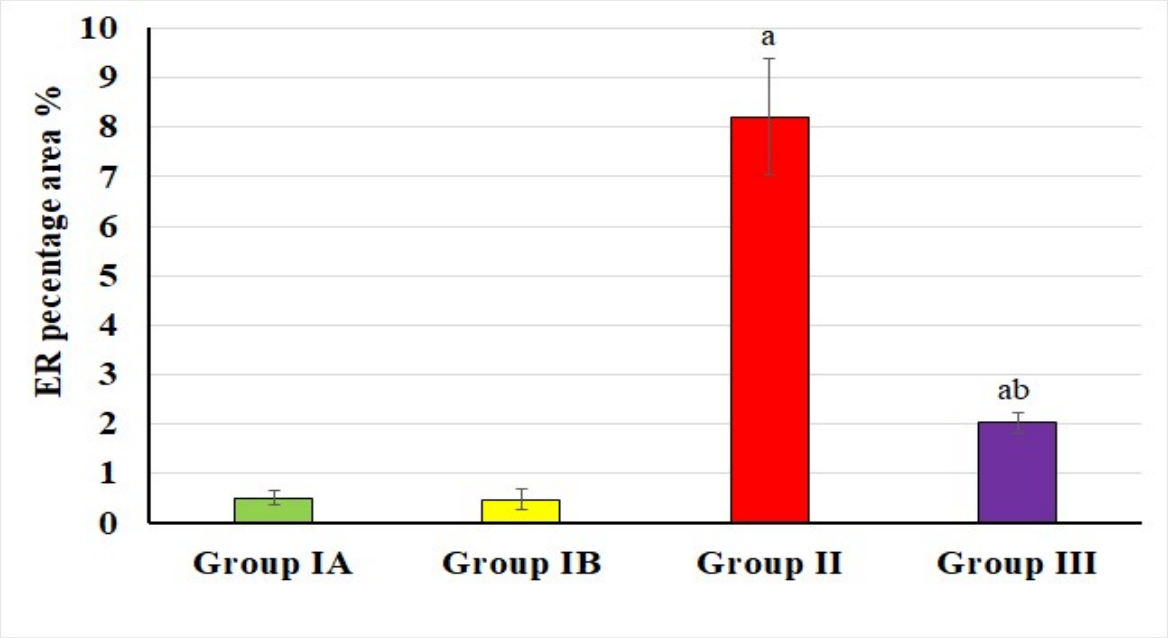

a: Significance relative to control group (IA & IB). b: Significance relative to group II (DMBA).

Histogram (1): Percentage (%) area of ER positive immune-reaction (mean±SD) in the control and experimental groups.

- **Percentage area of Ki-67 positive immune-reaction at a magnification x400 in the control and experimental groups:**

As regard the control group (I), subgroup IA (0.270 ± 0.06) and subgroup IB (0.268 ± 0.06) showed insignificant (P=1) difference in the percentage area of ki-67 positive immune-reaction. As compared to control group (IA and IB), a high significant increase in the percentage area of Ki-67 positive immune-reaction was noticed in group II (1.647 ± 0.28, P<0.001). Furthermore, a significant (P =0.001) increase in the percentage area of ki-67 positive immune-reaction was noticed in group III (0.655 ± 0.05), as compared to control group (IA and IB). In addition, group III showed a high

significant (P<0.001) decrease in the percentage area of Ki-67 positive immune-reaction, as compared to group II **(Table 2 and Histogram 2).**

Table (2): Percentage (%) area of Ki-67 positive immune-reaction (mean±SD) in the control and experimental groups:

	Group I (Control)		Group II (DMBA)	Group III (DMBA+ Paclitaxel)	Test of significance (ANOVA)
	Subgroup IA	Subgroup IB			
Mean ± SD	0.270 ± 0.06	0.268 ± 0.06	1.647 ± 0.28	0.655 ± 0.05	P < 0.001**
P_1		1.0	<0.001**	0.001*	
P_2			<0.001**	0.001*	
P_3				<0.001**	

6 replicas in each group, SD: Standard Deviation, P for ANOVA test.
* Statistically significant if P ≤0.05.
**Highly statistically significant result if P ≤0.001.
P_1: comparison in relation to group IA (Control).
P_2: comparison in relation to group IB (Control).
P_3: comparison in relation to group II (DMBA).

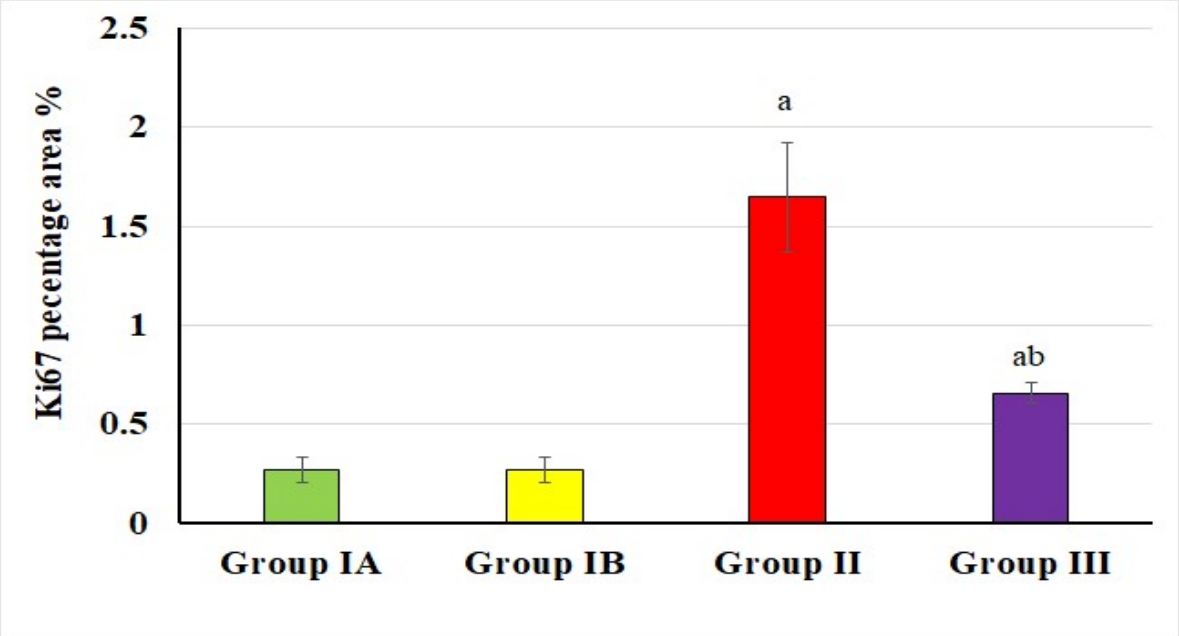

a: Significance relative to control group (IA & IB). b: Significance relative to group II (DMBA).

Histogram (2): Percentage (%) area of Ki-67 positive immune-reaction (mean±SD) in the control and experimental groups.

DISCUSSION:

The present study was designed to evaluate the histopathological and immunohistochemical changes induced by DMBA in the female rat mammary gland. As well as, we assessed the chemotherapeutic effect of paclitaxel. A multi-parametric approach was employed, including histopathological examination using (H&E), and immunohistochemical evaluation of ER, Ki-67 and HER2 expression.

Group II (DMBA-induced carcinogenesis) revealed intermediate-grade DCIS, high-grade DCIS and IDC. This histopathological pattern of DCIS and IDC is consistent with the DMBA-induced mammary carcinogenesis models that reported by **Hakkak et al** [25] and **Wibowo et al** [26]**.** DMBA is a potent chemical

carcinogen that requires metabolic activation by CYP1A1 and CYP1B1 enzymes to generate reactive metabolites capable of forming DNA adducts. These DNA lesions initiate genetic alterations that activate oncogenic signaling pathways involved in cell proliferation and survival. Furthermore, DMBA promotes oxidative stress and persistent inflammatory responses through activation of mediators such as NF-κB and COX-2, creating a tumor-promoting microenvironment that facilitates mammary carcinogenesis [27, 28]. Moreover, persistent oxidative stress further amplifies DNA damage and contributes to cancer progression [29].

Furthermore, DMBA produced uncontrolled proliferation of the ductal epithelial cells following disruption of the normal regulatory mechanisms governing cell growth and differentiation, representing an early event in mammary carcinogenesis [30]. Moreover, the neoplastic cells displayed evident nuclear pleomorphism, a hallmark of malignant transformation that reflects progressive genomic instability. The observed variation in nuclear size, shape, and chromatin organization is attributed to the accumulation of genetic and epigenetic alterations during tumor development. In addition, defects in DNA repair pathways together with persistent replication stress promote the emergence of genetically heterogeneous tumor cell populations [29,31]. Chromosomal instability resulting from abnormal mitotic spindle assembly and chromosome missegregation further contributes to nuclear atypia and structural abnormalities characteristic of malignant mammary tumors [32].

Group III (DMBA-induced carcinogenesis given paclitaxel) revealed that there was no evidence of IDC or DCIS and showed marked improvement of the tissue architecture. The therapeutic effect of paclitaxel is primarily attributed to its ability to stabilize microtubules through high-affinity binding to β-tubulin subunits. This interaction promotes microtubule polymerization while preventing their depolymerization, thereby disrupting the dynamic instability required for normal mitotic spindle function. Consequently, cancer cells undergo cell cycle arrest at the G2/M phase, leading to inhibition of uncontrolled cellular proliferation. In addition to its antimitotic activity, paclitaxel induces apoptosis through multiple molecular mechanisms. Persistent microtubule stabilization induces endoplasmic reticulum stress, promotes mitochondrial outer membrane permeabilization via the activation of BAX and BAK, resulting in cytochrome c release and subsequent caspase activation [33, 34]. Furthermore, paclitaxel has been reported to suppress survival signaling pathways, including the PI3K/Akt pathway, thereby enhancing the susceptibility of tumor cells to apoptosis [35].

The therapeutic potential of paclitaxel against DMBA-induced mammary carcinogenesis has been documented in several experimental studies. **Padmavathi et al**[16] reported that paclitaxel effectively attenuated oxidative stress by reducing lipid peroxidation while restoring the activities of antioxidant enzymes, as compared with the DMBA-treated group. Likewise, histopathological findings from another experimental study demonstrated that treatment with paclitaxel-loaded liposomes prevented malignant invasion and was associated with necrotic areas together with residual foci of DCIS, indicating a marked therapeutic response [36].

The high mortality associated with group II is consistent with the known potent carcinogenic activity of DMBA and its ability to induce invasive mammary carcinomas[37]. Paclitaxel treatment in group III improved the survival outcome with a lower mortality rate, but the mortality rate did not return to zero. This may be attributed to the well-documented systemic toxicity of paclitaxel, including myelosuppression, peripheral neuropathy, cardiotoxicity, hepatotoxicity and nephrotoxicity, which could compromise survival despite its antitumor activity [12].

In the present study, group II showed DCIS and IDC, which were ER, and Ki67 positive, but HER2 negative. This finding is consistent with the nature of DMBA-induced mammary tumor model, which develops a diverse assortment of mammary tumors with resemblance to human breast cancer subtypes [38]. Since Luminal tumors represent the most prevalent subtypes in human (60%-70 %) breast cancer and are predominantly HER2-negative [39], the emergence of HER2-negative tumors in the DMBA model is expected and reflects the biological heterogeneity of the model and its relevance to the clinical setting. However, some studies demonstrated HER2 positive reaction in DMBA induced carcinogenesis in rats. **Aisyah et al** [40], reported positive HER2 expression in DMBA-induced mammary tumors of the untreated positive control group, suggesting that HER2 positivity can occur in DMBA models independent of treatment.

In present study, group II showed a high significant increase in ER percentage area, as compared to the control group, consistent with the hormone-dependent nature of DMBA-induced mammary carcinogenesis. **Alvarado et al.**[41] suggested that the carcinogenic effect of DMBA is partly mediated through neuroendocrine disturbances, including enhanced preovulatory secretion of 17β-estradiol and prolactin. These hormonal changes promote the proliferation of hormone-sensitive mammary epithelial cells and emphasize the role of endocrine dysregulation in mammary tumor development. Such findings may explain the increased ER percentage area observed in the current study.

Paclitaxel chemotherapy in group III reduced ER percentage area high significantly, as compared to group II. The observed reduction in ER expression is most likely attributed to the cytotoxic activity of paclitaxel against rapidly proliferating tumor cells, including ER-positive cell populations. By binding to β-tubulin and stabilizing microtubules, paclitaxel disrupts mitotic spindle dynamics, resulting in prolonged mitotic arrest and subsequent apoptotic cell death. Therefore, the decline in ER expression is more likely a consequence of the selective elimination of ER-expressing tumor cells than a direct modulation of ER expression [42].

The current findings are consistent with previous experimental studies demonstrating enhanced ER expression in DMBA-induced mammary carcinogenesis. **Deepalakshmi and Mirunalini** [43] reported that mammary tumors induced by DMBA in female Sprague-Dawley rats exhibited ER expression, and that the chemopreventive effect of Pleurotus ostreatus was partly mediated through modulation of ER signaling. Likewise, **Helmy et al** [44] demonstrated a significant increase in ER expression following DMBA administration, whereas treatment with doxorubicin/folate-targeted trans-ferulic acid-loaded PLGA nanoparticles markedly reduced ER expression compared with untreated tumor-bearing animals**.**

In the current study, group II showed a high significant increase in Ki67 percentage area, as compared to control group. This is reflecting high proliferative activity. This finding is consistent with **Alvarado et al** [41]**,** who demonstrated that DMBA-induced mammary carcinogenesis in rats is mostly associated with a significant increase in Ki-67 expression. **Patel & Shah** [45]**,** confirmed that administration of DMBA resulted in a marked increase in Ki-67 expression in mammary tissues, whereas hesperidin treatment significantly reduced Ki-67 levels, indicating suppression of cell proliferation.

Paclitaxel administration in group III showed a high significant decrease in Ki-67 percentage area, as compared to group II. In addition, paclitaxel significantly decreased Ki-67 percentage area, as compared to control group. These findings agree with **Weaver** [33]**,** who reported that paclitaxel kills cancer cells through its anti-mitotic action, leading to suppression of proliferation.

CONCLUSION:

Paclitaxel ameliorated the DMBA-induced mammary carcinogenesis in female rats. The treatment resulted in significantly greater histopathological and immunohistochemical improvement, demonstrating a chemotherapeutic effect.

Author Contributions:

Conceptualization, technique, software validation, formal analysis, resource data curation, writing, original draught preparation, writing, review and editing Zeinab Mohamed Abd Elrahman, Dalia Abdelrahman Shabaan, **Email**: dalia_abdelrahman@mans.edu.eg, Amany Hassan Abdel-wahab Salama, **Email**: dramanyhassan@man.edu.eg, Shehab Hafez Mohamed, **Email**: shehabelashmawi@gmail.com, and Sanaa Ahmed El-Sherbiny, **Email**: drsanaaelsherbiny@gmail.com. The published version of the manuscript has been read by all authors, who have approved it.

Conflicts of Interest: The authors declare no conflict of interest.

REFERENCES:

1. Sung H, Ferlay J, Siegel RL, Laversanne M, Soerjomataram I, Jemal A, et al. Global Cancer Statistics 2020: GLOBOCAN Estimates of Incidence and Mortality Worldwide for 36 Cancers in 185 Countries. CA: A Cancer Journal for Clinicians. 2021;71(3):209-49.
2. Azim HA, Elghazawy H, Ghazy RM, Abdelaziz AH, Abdelsalam M, Elzorkany A, et al. Clinicopathologic Features of Breast Cancer in Egypt—Contemporary Profile and Future Needs: A Systematic Review and Meta-Analysis. JCO Global Oncology. 2023(9).
3. Salem MRH, Moneim Tewfik Chalabi NA, Boraei Mohammed AAG, Yacoub GEE. The Incidence of Breast Cancer in Egyptian Females in Correlation to Different Mammographic ACR Densities. QJM: An International Journal of Medicine. 2024;117(Supplement_2).
4. Hamdy SM, Sayed ON, Abdel Latif AKM, Abd-Elazeez AM, Amin AM. Protective Effect Of Hesperidin And Tiger Nut Against DMBA Carcinogenicity In Female Rats. Biochemistry Letters. 2016;11(1):150-67.
5. Naruse M, Ishigamori R, Imai T. The Unique Genetic and Histological Characteristics of DMBA-Induced Mammary Tumors in an Organoid-Based Carcinogenesis Model. Frontiers in Genetics. 2021;12.
6. Loo WTY, Cheung MNB, Loo PC. Meta-Analysis: 7,12-Dimethylbenz[a]anthracene (DMBA) Induces Diverse Types of Breast Carcinoma in Rat Models: A Systematic Review of Tumor Histopathology and Pathogenesis. World Journal of Biology Pharmacy and Health Sciences. 2025;24(2):354-9.
7. Alvarado A, Lopes AC, Faustino-Rocha AI, Cabrita AMS, Ferreira R, Oliveira PA, et al. Prognostic factors in MNU and DMBA-induced mammary tumors in female rats. Pathology - Research and Practice. 2017;213(5):441-6.
8. Nicotra R, Lutz C, Messal HA, Jonkers J. Rat Models of Hormone Receptor-Positive Breast Cancer. Journal of Mammary Gland Biology and Neoplasia. 2024;29(1).
9. Muley A, Navale A, Gupta R, Tekade RK. "Nano-Paclitaxel" Unlocking Potential and Redefining Cancer Chemotherapy. ACS Omega. 2025;10(27):28670-90.
10. Ozcelik B, Turkyilmaz C, Ozgun MT, Serin IS, Batukan C, Ozdamar S, et al. Prevention of paclitaxel and cisplatin induced ovarian damage in rats by a gonadotropin-releasing hormone agonist. Fertility and Sterility. 2010;93(5):1609-14.
11. Abu Samaan TM, Samec M, Liskova A, Kubatka P, Büsselberg D. Paclitaxel's Mechanistic and Clinical Effects on Breast Cancer. Biomolecules. 2019;9(12):789.
12. Naeem AG, Fawzi SF, Elmorsi RM, George MY. Paclitaxel-induced adverse effects: insights into multi-organ toxicities and molecular mechanisms. Naunyn-Schmiedeberg's archives of pharmacology. 2026;399(2):1721-50.
13. Nassan Mohamed A, Soliman Mohamed M, Ismail Shimaa A, El-Shazly S. Effect of Taraxacum officinale extract on PI3K/Akt pathway in DMBA-induced breast cancer in albino rats. Bioscience Reports. 2018;38(6).

14. Karimi B, Ashrafi M, Shomali T, Yektaseresht A. Therapeutic effect of simvastatin on DMBA-induced breast cancer in mice. Fundamental & Clinical Pharmacology. 2018;33(1):84-93.
15. Faheem HM, Elnbtete SM. Artemisia annua Extract Ameliorates DMBA-induced Breast Cancer in Albino rats; Antioxidant and Genetic Effects. Oriental Journal of Chemistry. 2020;36(03):451-7.
16. Padmavathi R, Senthilnathan P, Chodon D, Sakthisekaran D. Therapeutic effect of paclitaxel and propolis on lipid peroxidation and antioxidant system in 7,12 dimethyl benz(a)anthracene-induced breast cancer in female Sprague Dawley rats. Life Sciences. 2006;78(24):2820-5.
17. Luo M, Chen P-p, Yang L, Wang P, Lu Y-l, Shi F-g, et al. Sodium ferulate inhibits myocardial hypertrophy induced by abdominal coarctation in rats: Involvement of cardiac PKC and MAPK signaling pathways. Biomedicine & Pharmacotherapy. 2019;112:108735.
18. Bancroft JD, Layton C. The hematoxylins and eosin. Bancroft's Theory and Practice of Histological Techniques: Elsevier; 2019. p. 126-38.
19. Maaruf NA, Najjar SM, Ali SA. Anatomical and Histopathological Comparative Studies Between Right and Left Mammary Tumors in a Rat Model Induced by DMBA. Pakistan Veterinary Journal. 2023;43(2).
20. Sanderson T, Wild G, Cull AM, Marston J, Zardin G. Immunohistochemical and immunofluorescent techniques. Bancroft's Theory and Practice of Histological Techniques: Elsevier; 2019. p. 337-94.
21. Yu K, Huang Z-Y, Xu X-L, Li J, Fu X-W, Deng S-L. Estrogen Receptor Function: Impact on the Human Endometrium. Frontiers in Endocrinology. 2022;13.
22. Dame MK, Jiang Y, Appelman HD, Copley KD, McClintock SD, Aslam MN, et al. Human colonic crypts in culture: segregation of immunochemical markers in normal versus adenoma-derived. Laboratory Investigation. 2014;94(2):222-34.
23. Rakha EA, Pinder SE, Bartlett JMS, Ibrahim M, Starczynski J, Carder PJ, et al. Updated UK Recommendations for HER2 assessment in breast cancer. Journal of Clinical Pathology. 2014;68(2):93-9.
24. Hazra A, Gogtay N. Biostatistics series module 3: Comparing groups: Numerical variables. Indian Journal of Dermatology. 2016;61(3):251.
25. Hakkak R, Holley AW, MacLeod SL, Simpson PM, Fuchs GJ, Jo CH, et al. Obesity promotes 7,12-dimethylbenz(a)anthracene-induced mammary tumor development in female zucker rats. Breast Cancer Research. 2005;7(5).
26. Wibowo AE, Sriningsih S, Wuyung PE, Ranasasmita R. The Influence of DMBA (7,12-dimethylbenz-[a]anthracene) Regimen In The Development of Mammae Carcinogénesis on Sprague Dawley Female Rat. Indonesian Journal of Cancer Chemoprevention. 2010;1(1):60.
27. Pratama DAOA, Cahyati AN, Kustiati U, Hardian AB, Permata FS. Proteomics analysis of carcinogenesis in a rat model of mammary cancer induced by DMBA (7,12-dimethylbenz[a]anthracene). F1000Research. 2024;12:606.
28. Zingué S, Tchoupang EN, Madji LT, Pehuie Fomat BH, Mafogang B, Njamen D, et al. Ricinodendron heudelotii (Euphorbiaceae) seed oil prevents DMBA-induced breast cancer under menopause-like conditions in Wistar rats. Frontiers in Pharmacology. 2024;15.
29. Hanahan D. Hallmarks of Cancer: New Dimensions. Cancer Discovery. 2022;12(1):31-46.
30. Mumtaz S, Ali S, Pervaiz A, Ahmad F, Latif AA, Khan MN, et al. Biochemical and Histopathological Impact of DMBA-Induced Breast Cancer and Therapeutic Potential of Silk Sericin and Sericin Silver Nanoparticles. Microscopy Research and Technique. 2025;88(10):2675-89.
31. Zack TI, Schumacher SE, Carter SL, Cherniack AD, Saksena G, Tabak B, et al. Pan-cancer patterns of somatic copy number alteration. Nature Genetics. 2013;45(10):1134-40.
32. Bakhoum SF, Cantley LC. The Multifaceted Role of Chromosomal Instability in Cancer and Its Microenvironment. Cell. 2018;174(6):1347-60.
33. Weaver BA. How Taxol/paclitaxel kills cancer cells. Molecular Biology of the Cell. 2014;25(18):2677-81.
34. Sati P, Sharma E, Dhyani P, Attri DC, Rana R, Kiyekbayeva L, et al. Paclitaxel and its semi-synthetic derivatives: comprehensive insights into chemical structure, mechanisms of action, and anticancer properties. European Journal of Medical Research. 2024;29(1).
35. Dong Z, Zhang D, Yang R, Wang S. Paclitaxel: new uses for an old drug. Drug Design, Development and Therapy. 2014:279.
36. Shaban N, Abdel-Rahman S, Haggag A, Awad D, Bassiouny A, Talaat I. Combination between Taxol-Encapsulated Liposomes and Eruca sativa Seed Extract Suppresses Mammary Tumors in Female Rats Induced by 7,12 Dimethylbenz(α)anthracene. Asian Pacific Journal of Cancer Prevention. 2016;17(1):117-23.
37. Zingue S, Mindang ELN, Awounfack FC, Kalgonbe AY, Kada MM, Njamen D, et al. Oral administration of tartrazine (E102) accelerates the incidence and the development of 7,12-dimethylbenz(a) anthracene (DMBA)-induced breast cancer in rats. BMC Complementary Medicine and Therapies. 2021;21(1).
38. Schulte AJ, Andrechek ER. Insights from Genomic Sequencing of Preclinical Breast Cancer Models Establish Human Parallels to Increase Therapeutic Applicability. Journal of Mammary Gland Biology and Neoplasia. 2026;31(1).
39. Johnson KS, Conant EF, Soo MS. Molecular Subtypes of Breast Cancer: A Review for Breast Radiologists. Journal of Breast Imaging. 2020;3(1):12-24.
40. Aisyah S, Handharyani E, Bermawie N, Setiyono A. Effects of ethanol extract of curry leaves (Murraya koenigii) on HER2 and caspase-3 expression in rat model mammary carcinoma. Veterinary World. 2021:1988-94.
41. Alvarado A, Faustino-Rocha AI, Colaço B, Oliveira PA. Experimental mammary carcinogenesis - Rat models. Life Sciences. 2017;173:116-34.

42. Qin X, Presser A, Johnson L, Matoba Y, Shay BS, Xu W, et al. Paclitaxel-induced mitotic arrest results in a convergence of apoptotic dependencies that can be safely exploited by BCL-XL degradation to overcome cancer chemoresistance. openRxiv; 2025.
43. Deepalakshmi K, Mirunalini S. Efficacy of Pleurotus ostreatus (Jacq. Ex Fr.) P.kumm. on 7,12-dimethylbenz(a)anthracene induced mammary carcinogenesis in female Sprague-Dawley rats. European Journal of Molecular & Clinical Medicine. 2016;3(2):73.
44. Helmy SA, El-Mofty S, El Gayar AM, El-Sherbiny IM, El-Far YM. Novel doxorubicin / folate-targeted trans-ferulic acid-loaded PLGA nanoparticles combination: In-vivo superiority over standard chemotherapeutic regimen for breast cancer treatment. Biomedicine & Pharmacotherapy. 2022;145:112376.
45. Patel P, Shah J. Protective effects of hesperidin through attenuation of Ki67 expression against DMBA-induced breast cancer in female rats. Life Sciences. 2021;285:119957.